Extracting the longitudinal structure function $F_L(x,Q^2)$ at small x from a Froissart-bounded parametrization of $F_2(x,Q^2)$

L. P. Kaptari,[1,2] A. V. Kotikov,[1,2] N. Yu. Chernikova,[3] and Pengming Zhang[1,4]

[1]*Institute of Modern Physics, Chinese Academy of Science, 509 Nanchang Road, 730000 Lanzhou, China*
[2]*Bogoliubov Laboratory of Theoretical Physics, Joint Institute for Nuclear Research, Dubna 141980, Russia*
[3]*Sunday school, Dubna 141980, Russia*
[4]*University of Chinese Academy of Sciences, Yuquanlu 19A, Beijing 100049, China*

(Received 10 April 2019; published 21 May 2019)

We present a method to extract, in the leading- and next-to-leading-order approximations, the longitudinal deep inelastic scattering structure function $F_L(x,Q^2)$ from the experimental data by relying on a Froissart-bounded parametrization of the transversal structure function $F_2(x,Q^2)$ and, partially, on the Dokshitzer-Gribov-Lipatov-Altarelli-Parisi equations. Particular attention is paid to the kinematics of low and ultralow values of the Bjorken variable x, $x \sim 10^{-5}$–10^{-2}. Analytical expressions for $F_L(x,Q^2)$ in terms of the effective parameters of the parametrization of $F_2(x,Q^2)$ are presented explicitly. We argue that the obtained structure functions $F_L(x,Q^2)$ within both, the leading- and next-to-leading-order approximations, manifestly obey the Froissart boundary conditions. Numerical calculations and comparison with available data from the ZEUS and H1 collaborations at HERA demonstrate that the suggested method provides reliable structure functions $F_L(x,Q^2)$ at low x in a wide range of the momentum transfer ($1\ \mathrm{GeV}^2 < Q^2 < 3000\ \mathrm{GeV}^2$) and can be applied as well in analyses of ultrahigh-energy processes with cosmic neutrinos.

DOI: 10.1103/PhysRevD.99.096019

I. INTRODUCTION

At small values of the Bjorken variable x, the nonperturbative effects in the deep inelastic structure functions (SFs) were expected to play a decisive role in describing the corresponding cross sections. However, it has been observed, cf. Ref. [1], that even in the region of low momentum transfer $Q^2 \sim 1\ \mathrm{GeV}^2$, where traditionally the soft processes were considered to govern the cross sections, the perturbative QCD (pQCD) methods could still adequately describe high-energy processes, in particular, at relatively low values of x: $10^{-5} \leq x \leq 10^{-2}$. This has been clearly demonstrated in early analyses of the *pre*-HERA data within approaches based on pQCD and on the idea that the steep behavior of the momentum distributions at low x can be generated purely dynamically, merely from measured valence densities, by utilizing QCD evolution equations [2]. This idea has been confirmed by subsequent measurements of the structure function $F_2(x,Q^2)$ at $x > 10^{-2}$. At smaller $x < 10^{-2}$, to achieve a better agreement with data, the dynamical parton distribution functions (PDFs) require additional fine-tuning of the valence-like input parameters [3,4]. Such complementary tuning results in rather stable parametrizations of PDFs in a broad range of Q^2 [5]. Furthermore, there are various groups (cf. Refs. [4,6] and references therein) actively involved in extracting PDFs from experimental data, with particular attention paid to the description of low-x HERA and LHC data (cf. Refs. [7–9]). In most cases the extraction procedure is supplemented by the small-x Balitsky-Fadin-Kuraev-Lipatov (BFKL) resummation [10] of the evolution equations and deep inelastic scattering (DIS) coefficient functions, thereby leading to resummed PDF sets (for recent reviews see, for example, Refs. [7,8]). It has been shown, that the inclusion of BFKL resummation significantly improves the quantitative description of the small-x and small-Q^2 HERA data, in particular in the next-to-leading-order (NLO) and next-to-next-to-leading-order (NNLO) approximations, for both the inclusive and the charm structure functions. The resummation of logarithms at low x also stabilizes the perturbative expansion, and the resulting PDFs receive a specific shape, rising at small x.

It should also be noted that, at ultralow x, $x \to 0$, the pQCD evolution, leads, nonetheless, to a rather singular behavior of PDFs (see e.g., Ref. [11] and references therein quoted), which is in strong disagreement with the Froissart boundary conditions [12]. In Refs. [13–15] M. M. Block *et al.* have suggested a new parametrization of the SF

$F_2(x, Q^2)$ which describes fairly well the available experimental data on the reduced cross sections and, at asymptotically low x, provides a behavior of the hadron-hadron cross sections $\sim \ln^2 s$ at large s, where s is the Mandelstam variable denoting the square of the total invariant energy of the process, in full accordance with the Froissart predictions [12]. The most recent parametrization suggested in Ref. [15] by Block, Durand and Ha—referred to here as the BDH parametrization—is also pertinent in investigations of lepton-hadron processes at ultrahigh energies, e.g., the scattering of cosmic neutrinos from hadrons [14–18]. Note that, in the case of neutrino scattering other SFs, such as the pure valence SF $F_3(x, Q^2)$, and longitudinal SF $F_L(x, Q^2)$, are relevant to describe the process. While at low values of x the valence structure function $F_3(x, Q^2)$ vanishes, the longitudinal SF $F_L(x, Q^2)$ remains finite and can even be predominant in the cross section. Thus, a theoretical analysis of the longitudinal SF $F_L(x, Q^2)$ at low x, in the context of the fulfilment of the Froissart prescriptions, is of great importance in treatments of ultrahigh energy processes as well.

Hitherto, most theoretical analyses [17,19] of neutrino processes have been performed in the leading-order (LO) approximation, within which the Callan-Gross relation is assumed to be satisfied exactly, i.e., the longitudinal structure function $F_L = 0$. Beyond the LO the effects from F_L can be sizable, and hence it can no longer be neglected, cf. Refs. [17,20].

In the present paper we present a method of extraction of the longitudinal SF, $F_L(x, Q^2)$ in the kinematical region of low values of the Bjorken variable x from the known structure function $F_2^{\rm BDH}(x, Q^2)$ and known derivative $dF_2^{\rm BDH}/d\ln(Q^2)$ by relying, to some extent, on the Dokshitzer-Gribov-Lipatov-Altarelli-Parisi (DGLAP) Q^2-evolution equations [21]. In our calculations we use the most recent version of the BDH parametrization reported in Ref. [15]. In fact, the presented approach is a further development of the methods previously suggested in Refs. [22,23] to extract some general characteristics of the gluon density and longitudinal SF at low x from the experimentally known SF $F_2(x, Q^2)$ and logarithmic derivative $dF_2/d\ln Q^2$. The extraction procedure was inspired by the Altarelli-Martinelli formula [24] used to determine the gluon density from $F_L(x, Q^2)$, and improved upon in Ref. [25].

In our case, the SF $F_2(x, Q^2)$ is considered experimentally known as it is defined by the $F_2^{\rm BDH}(x, Q^2)$ parametrization [15], i.e., the x and Q^2 dependencies of the transverse SF and the corresponding logarithmic derivative are supposed to be known. As a first step of the analysis, the method has been applied to extract $F_L(x, Q^2)$ in the LO. The results of such a procedure have been briefly reported in Ref. [26], where it has been demonstrated that the extracted structure function $F_L^{\rm BDH}(x, Q^2)$ at moderate and low values of x is in reasonably good agreement with the available experimental data [27]. However, for ultralow values of x the agreement becomes less satisfactory and even rather poor in the limit $x \to 0$. This serves as a clear indication that the LO analysis is not sufficient in the region $x \to 0$ and the NLO corrections become significant and are to be implemented in the extraction procedure. Similar investigations of the longitudinal SF have been performed in Ref. [28].

In this paper, we present in some detail the LO analysis [26], and provide further development of the method by extending it beyond the LO approximation by considering and resumming the NLO corrections.

It is worth emphasizing that the NLO approximation for $F_L(x, Q^2)$, i.e., calculations up to α_s^2 corrections, corresponds to the NNLO approximation for $F_2(x, Q^2)$ which, in the LO, is $\propto \alpha_s^0$. Hence, in our approach it becomes possible to perform NLO and NNLO analyses of the ultrahigh-energy ($\sqrt{s} \sim 1$ TeV) neutrino cross sections similar to existing NLO [29] and NNLO [30] investigations based on pQCD. Such analyses are rather important in view of the recently arosed possibility of a direct comparison with emerging data from the IceCube Collaboration [31] (cf. also Ref. [32]) and anticipated data from IceCube-Gen2 [33], whose performance will be much better and which is expected to provide substantially more precise measurements of the neutrino-nucleon cross section.

Our paper is organized as follows.

In Sec. II we present the basic formulas of the approach. The relevant system of equations to be used in the extraction of the longitudinal SF, together with the corresponding splitting functions and coefficient functions are displayed explicitly. In Secs. II A and II B we discuss the Mellin transforms of the transversal and longitudinal SFs in the LO and NLO approximations for momenta corresponding to low x. Explicit expressions for the anomalous dimensions and Wilson coefficients in the LO for low x are given as well.

In Sec. III we write down the details of obtaining all of the quantities related to the BDH parametrization [15] needed in the subsequent calculations, such as the corresponding derivatives and Mellin transforms within the considered kinematics and approximations. The next two sections, Secs. IV and V, are entirely devoted to the description of the gist of the mathematical methods and manipulations used to calculate the Mellin transforms and their inverses to find the longitudinal SF in the LO (Sec. IV) and NLO (Sec. V) approximations. Numerical results for the extracted $F_L(x, Q^2)$ in the LO and NLO, together with comparisons with the experimental data from the H1 Collaboration, are presented in Sec. VI, where we discuss the Q^2 and x dependencies of the extracted SF $F_L(x, Q^2)$ and the ratio $R_L(x, Q^2)$ of the longitudinal to transversal cross sections within the LO and NLO approximations. Conclusions and a summary are given in Sec. VII. The most cumbersome expressions are relegated to Appendices A and B.

II. BASIC FORMULAS

In view of the fact that at low values of x the nonsinglet quark distributions become negligibly small in comparison with the singlet distributions, in the present analysis they are disregarded. Then, the transverse SF $F_2(x,Q^2)$ and longitudinal SF $F_L(x,Q^2)$ are expressed solely via the singlet quark and gluon densities $xf_a(x,Q^2)$ (hereafter $a=s,\,g$ and $k=2,\,L$) as

$$F_k(x,Q^2)=e\sum_{a=s,g}[B_{k,a}(x)\otimes xf_a(x,Q^2)], \qquad (1)$$

where e is the average charge squared, $e=\frac{1}{f}\sum_{i=1}^{f}e_i^2\equiv\frac{e_{2f}}{f}$ where f is the number of considered flavors, and $q^2=-Q^2$ and $x=Q^2/2pq$ (with p being the momentum of the nucleon) denote the momentum transfer and the Bjorken scaling variable, respectively. The quantities $B_{k,a}(x)$ are the known Wilson coefficient functions. In Eq. (1) and throughout the rest of the paper, the symbol $\otimes$ is used to denote the convolution formula, i.e., $f_1(x)\otimes f_2(x)\equiv\int_x^1\frac{dy}{y}f_1(y)f_2(\frac{x}{y})$.

According to the DGLAP Q^2-evolution equations [21] the leading-twist quark, $xf_s(x,Q^2)$, and gluon, $xf_g(x,Q^2)$, distributions obey the following system of integro-differential equations:

$$\frac{d(xf_a(x,Q^2))}{d\ln Q^2}=-\frac{1}{2}\sum_{a,b=s,g}P_{ab}^{(0)}(x)\otimes xf_b(x,Q^2), \qquad (2)$$

where $P_{ab}(x)$ ($a,\,b=s,\,g$) are the corresponding splitting functions.

Within pQCD, and up to the NLO corrections, the coefficient functions $B_{k,a}(x)$ and the splitting functions $P_{ab}(x)$ read as

$$B_{2,s}(x)=\delta(1-x)+a_s(Q^2)B_{2,s}^{(1)}(x), \qquad (3)$$

$$B_{2,g}(x)=a_s(Q^2)B_{2,g}^{(1)}(x), \qquad (4)$$

$$B_{L,a}(x)=a_s(Q^2)B_{L,a}^{(0)}(x)+a_s^2(Q^2)B_{L,a}^{(1)}(x), \qquad (5)$$

$$P_{a,b}(x)=a_s(Q^2)P_{a,b}^{(0)}(x)+a_s^2(Q^2)P_{a,b}^{(1)}(x), \qquad (6)$$

where $a_s(Q^2)=\alpha_s(Q^2)/4\pi$ is the QCD running coupling, which, for convenience, includes in its definition an additional factor of 4π in comparison with the standard notation. In the above equations and hereafter the superscripts (0, 1) mark the corresponding order of the perturbation theory: (0) for LO and (1) for NLO.

By inserting Eqs. (3)–(6) into Eqs. (1) and (2) the final NLO system of equations for the desired PDFs becomes

$$\frac{d(xf_g(x,Q^2))}{d\ln Q^2}=-\frac{a_s(Q^2)}{2}[(P_{gg}^{(0)}(x)+a_s(Q^2)\tilde{P}_{gg}^{(1)}(x))\otimes xf_g(x,Q^2)+e^{-1}(P_{gs}^{(0)}(x)+a_s(Q^2)\tilde{P}_{gs}^{(1)}(x))\otimes F_2(x,Q^2)+O(a_s^3)] \qquad (7)$$

$$\frac{dF_2(x,Q^2)}{d\ln Q^2}=-\frac{a_s(Q^2)}{2}[e(P_{sg}^{(0)}(x)+a_s(Q^2)\tilde{P}_{sg}^{(1)}(x))\otimes xf_g(x,Q^2)+(P_{ss}^{(0)}(x)+a_s(Q^2)\tilde{P}_{ss}^{(1)}(x))\otimes F_2(x,Q^2)+O(a_s^3)], \qquad (8)$$

$$F_L(x,Q^2)=a_s(Q^2)[e(B_{L,g}^{(0)}(x)+\tilde{B}_{L,g}^{(1)}(x))\otimes xf_g(x,Q^2)+(B_{L,q}^{(0)}(x)a_s(Q^2)\tilde{B}_{L,q}^{(1)}(x))\otimes F_2(x,Q^2)+O(a_s^3)], \qquad (9)$$

where, for brevity, the following notations have been employed:

$$\tilde{P}_{sg}^{(1)}(x)=P_{sg}^{(1)}(x)+B_{2,s}^{(1)}(x)\otimes P_{sg}^{(0)}(x)+B_{2,g}^{(0)}(x)\otimes(2\beta_0\delta(1-x)+P_{gg}^{(0)}(x)-P_{ss}^{(0)}(x)),$$
$$\tilde{P}_{ss}^{(1)}(x)=P_{ss}^{(1)}(x)+2\beta_0B_{2,s}^{(1)}(x)\otimes\delta(1-x)+B_{2,g}^{(1)}(x)\otimes P_{gq}^{(0)}(x),$$
$$\tilde{P}_{gs}^{(1)}(x)=P_{gs}^{(1)}(x)-B_{2,s}^{(1)}(x)\otimes P_{gs}^{(0)}(x),\qquad \tilde{P}_{gg}^{(1)}(x)=P_{gg}^{(1)}(x)-B_{2,g}^{(1)}(x)\otimes P_{gs}^{(0)}(x), \qquad (10)$$

$$\tilde{B}_{L,g}^{(1)}(x)=B_{L,g}^{(1)}(x)-B_{2,g}^{(1)}(x)\otimes B_{L,g}^{(0)}(x),\qquad \tilde{B}_{L,s}^{(1)}(x)=B_{L,s}^{(1)}(x)-B_{2,s}^{(1)}(x)\otimes B_{L,s}^{(0)}(x) \qquad (11)$$

where β_0 and β_1 are the first two coefficients of the QCD β function

$$\beta_0=\frac{1}{3}(11C_A-2f),\qquad \beta_1=\frac{1}{3}(34C_A^2-2f(5C_A+3C_F)). \qquad (12)$$

In Eq. (12) $C_F=(N_c^2-1)/(2N_c)$ and $C_A=N_c$ are the Casimir operators in the fundamental and adjoint representations of the $SU(N_c)$ color group, respectively. Within QCD $N_c=3$, and hence $C_F=4/3$ and $C_A=3$.

A few remarks are in order here. As is known [34,35], Eq. (7) in its actual form leads to a too singular behavior of the gluon distribution at small x, violating the Froissart boundary restrictions. One can go beyond the perturbative theory and try to cure the problem by adding to the rhs of Eq. (7) terms proportional to $(xf_g)^2$ which make the distribution (and hence, the corresponding cross sections [36]) less singular at the origin and can, in principle, reconcile it with the Froissart requirements. A detailed inspection of Eq. (7) in the context of the implementation of additional modifications to fulfill the Froissart conditions is beyond the scope of the present paper and in what follows we omit it in our analysis. However, the gluon distribution originating from the omitted Eq. (7) and entering into the remaining equations (8) and (9) is supposed to have the correct asymptotic behavior, i.e., to be of the same LO form as the BDH parametrization of $F_2^{\rm BDH}(x,Q^2)$. This conjecture has been confirmed in a previous analysis [37] where the early parametrization of $F_2(x,Q^2)$ [14] has been employed to determine the gluon density within the LO. Then, Eq. (8) with the known $F_2^{\rm BDH}(x,Q^2)$, can be considered as the definition of the gluon density $xf_g^{\rm BDH}(x,Q^2)$ in the whole kinematical interval, cf. Ref. [37]. Consequently, in the system (8)–(9) of two equations with two unknown distributions one can eliminate the gluon part and solve the remaining equation with respect to the longitudinal $F_L(x,Q^2)$ and express it via the known parameterization of $F_2(x,Q^2)$. With these statements, now we are in a position to solve Eqs. (8) and (9) and to extract the desired longitudinal SF. Notice that, although at first glance the above equations are relatively simple, directly solving Eqs. (8) and (9) actually turns out to be a rather complicated and cumbersome procedure. One can substantially simplify the calculations by considering Eqs. (8) and (9) in the space of Mellin momenta, and taking advantage of the fact that the convolution form $f_1(x)\otimes f_2(x)$ in x space becomes merely a product of individual Mellin transforms of the corresponding functions in the space of Mellin momenta. Consequently, all of our further calculations are performed in Mellin space.

A. Mellin transforms

The Mellin transform of the PDFs entering into Eqs. (8) and (9) are defined as

$$M_k(n,Q^2) = \int_0^1 dx x^{n-2} F_k(x,Q^2),$$
$$M_a(n,Q^2) = \int_0^1 dx x^{n-1} f_a(x,Q^2), \tag{13}$$
$$\gamma_{ab}^{(i)}(n) = \int_0^1 dx x^{n-2} P_{ab}^{(i)}(x),$$
$$B_{k,a}^{(i)}(n) = \int_0^1 dx x^{n-2} B_{k,a}^{(i)}(x), \tag{14}$$

where, as before, $a, b = s, g$ and $k = 2, L$. Then, after some algebra, the Mellin transforms of Eqs. (8) and (9) read as

$$\frac{dM_2(n,Q^2)}{d\ln Q^2} = -\frac{a_s(Q^2)}{2}[e(\gamma_{sg}^{(0)}(n)+a_s(Q^2)\tilde{\gamma}_{sg}^{(1)}(n)) \times M_g(n,Q^2)+(\gamma_{ss}^{(0)}(n) + a_s(Q^2)\tilde{\gamma}_{ss}^{(1)}(n))M_2(x,Q^2)+O(a_s^3)], \tag{15}$$

$$M_L(n,Q^2) = a_s(Q^2)[e(B_{L,g}^{(0)}(n)+a_s(Q^2)\tilde{B}_{L,g}^{(1)}(n))M_g(x,Q^2) +(B_{L,s}^{(0)}(n)+a_s(Q^2)\tilde{B}_{L,s}^{(1)}(n))M_2(x,Q^2) +O(a_s^3)], \tag{16}$$

where the anomalous dimensions $\gamma_{ab}^{(i)}(n)$ and the Wilson coefficients $B_{L,a}^{(i)}(n)$ $(i = 0,\, 1)$ are

$$\tilde{\gamma}_{sg}^{(1)}(n) = \gamma_{sg}^{(1)}(n) + B_{2,s}^{(1)}(n)\gamma_{sg}^{(0)}(n) + B_{2,g}^{(0)}(n)(2\beta_0 + \gamma_{gg}^{(0)}(n) - \gamma_{ss}^{(0)}(n)),$$
$$\tilde{\gamma}_{ss}^{(1)}(n) = \gamma_{ss}^{(1)}(x) + 2\beta_0 B_{2,s}^{(1)}(n) + B_{2,g}^{(1)}(n)\gamma_{gq}^{(0)}(n),$$

$$\tilde{\gamma}_{gs}^{(1)}(n) = P_{gs}^{(1)}(n) - B_{2,s}^{(1)}(n)\gamma_{gs}^{(0)}(x),$$
$$\tilde{\gamma}_{gg}^{(1)}(n) = \gamma_{gg}^{(1)}(n) - B_{2,g}^{(1)}(n)\gamma_{gs}^{(0)}(n), \tag{17}$$

$$\tilde{B}_{L,g}^{(1)}(n) = B_{L,g}^{(1)}(n) - B_{2,g}^{(1)}(n)B_{L,g}^{(0)}(n),$$
$$\tilde{B}_{L,s}^{(1)}(n) = B_{L,s}^{(1)}(n) - B_{2,s}^{(1)}(n)B_{L,s}^{(0)}(n). \tag{18}$$

The explicit expressions for the anomalous dimensions $\gamma_{ab}^{(i)}(n)$ $(i = 0, 1)$ and the LO Wilson coefficients $B_{L,a}^{(0)}(n)$ can be found in Ref. [38], whereas the NLO part, $B_{L,NS}^{(1)}(n)$ and $B_{L,a}^{(1)}(n)$, has been reported, for the first time, in Refs. [39,40]. Unfortunately, there are several misprints in the above-mentioned references. Errata for Refs. [39,40] can be found in, e.g., Ref. [41]. Yet, in Ref. [38] a factor of 2 in the LO coefficients $B_{L,a}^{(0)}(n)$ was missed. Observe that as mentioned above, the Mellin transform significantly simplifies our calculations for, the complicated integro-differential system of equations (8)–(9) in x space, is translated into a relatively simple system (15)–(16) of pure algebraic equations. Now, we solve the system (15)–(16) with respect to the longitudinal Mellin momentum $M_L(n,Q^2)$ and express it through the known momentum $M_2(x,Q^2)$ and the derivative $dM_2(n,Q^2)/d\ln Q^2$

$$M_L(n,Q^2) = -2\frac{B_{L,g}^{(0)}(n) + a_s(Q^2)\tilde{B}_{L,g}^{(1)}(n)}{\gamma_{sg}^{(0)}(n) + a_s(Q^2)\tilde{\gamma}_{sg}^{(1)}(n)}\frac{dM_2(n,Q^2)}{d\ln Q^2} + \left[(B_{L,s}^{(0)}(n) + a_s(Q^2)\tilde{B}_{L,s}^{(1)}(n)) - (B_{L,g}^{(0)}(n) + a_s(Q^2)\tilde{B}_{L,g}^{(1)}(n)) \times \frac{\gamma_{ss}^{(0)}(n) + a_s(Q^2)\tilde{\gamma}_{ss}^{(1)}(n)}{\gamma_{sg}^{(0)}(n) + a_s(Q^2)\tilde{\gamma}_{sg}^{(1)}(n)}\right] M_2(x,Q^2) + O(a_s^3). \tag{19}$$

B. Anomalous dimensions and coefficient functions

Here we present the explicit expressions for the LO ingredients only. The corresponding expressions for the NLO corrections are rather cumbersome and, as already mentioned, can be found in Refs. [38–41]. Explicitly, the LO anomalous dimensions $\gamma_{ab}^{(0)}(n)$ and the Wilson coefficients $B_{L,a}^{(0)}(n)$, are as follows:

$$\gamma_{sg}^{(0)}(n) = -\frac{4f(n^2+n+2)}{n(n+1)(n+2)},$$
$$\gamma_{ss}^{(0)}(n) = 8C_F\left[S_1(n) - \frac{3}{4} - \frac{1}{2n(n+1)}\right], \tag{20}$$

$$\gamma_{ga}^{(0)}(n) = -\frac{4C_F(n^2+n+2)}{(n-1)n(n+1)},$$
$$\gamma_{ss}^{(0)}(n) = 8C_A\left[S_1(n) - \frac{1}{(n-1)n} - \frac{1}{(n+1)(n+2)}\right] + 2\beta_0,$$
$$B_{L,g}^{(0)}(n) = \frac{8f}{(n+1)(n+2)}, \quad B_{L,q}^{(0)}(n) = \frac{4C_F}{(n+1)}. \tag{21}$$

In Eqs. (20) and (21) we introduce, and shall widely use throughout the rest of the paper, the notion of the so-called nested sums, defined as

$$S_{\pm i}(n) = \sum_{m=1}^{n} \frac{(\pm 1)^m}{m^i}, \quad S_{\pm i,j}(n) = \sum_{m=1}^{n} \frac{(\pm 1)^m}{m^i} S_j(m). \tag{22}$$

Note that in previous calculations [38–40] the notion of the nested sums (22) was not incorporated. Instead, other notations related to the nested sums of negative indices have been used

$$S'_m\left(\frac{n}{2}\right) = 2^{m-1}(S_m(n) + S_{-m}(n)),$$
$$\tilde{S}_m(n) = S_{-2,1}(n) \text{ (Ref. [38])},$$
$$K_m(n) = -S_{-m}(n),$$
$$Q(n) = -S_{-2,1}(n) \text{ (Refs. [39, 40])}. \tag{23}$$

Coming back to the Mellin transforms (15), (16) and (19), we recall that we are interested in investigation of the PDFs in the region of low x. In Mellin space it corresponds to small momenta, and at extremely low x, it suffices to restrict the analysis to the first momentum and to study the solutions of Eqs. (15), (16) and (19) for $n = 1 + \omega$ at $\omega \to 0$. The nested sums $S_m(n)$ (here n is not necessarily an integer) for positive indices m can be expressed via the familiar Riemann Ψ functions $\Psi(n)$ as

$$S_1(n) = \Psi(n+1) - \Psi(1),$$
$$S_m(n) = \zeta_m - \sum_{l=0}^{\infty} \frac{1}{(n+l+1)^m}, \quad (m > 1), \tag{24}$$

where ζ_m are Euler constants and the last series on the rhs of Eq. (24) is related to the mth derivative of the Ψ function.

A more complicated situation occurs for negative indices $m < 0$ for which the analytical continuation of the nested sums depends on the parity of the starting value of n. Since the anomalous dimensions (20) have been calculated for even n, in what follows we employ the analytical continuation of $S_{-m}(n)$ and $S_{-m,k}(n)$ starting from even values of n. The result is [42]

$$S_1(n) = -\ln 2 - \sum_{l=0}^{\infty} \frac{(-1)^{l+1}}{n+l+1},$$
$$S_{-m}(n) = \zeta_{-m} - \sum_{l=0}^{\infty} \frac{(-1)^{l+1}}{(n+l+1)^m} \, (m \geq 2),$$
$$\zeta_{-m} = (1 - 2^{-m})\zeta_m,$$
$$S_{-m,k}(n) = \sum_{l=0}^{\infty} \frac{(-1)^{l+1}}{(l+1)^m} S_k(l+1) - \sum_{l=0}^{\infty} \frac{(-1)^{l+1}}{(n+l+1)^m} S_k(n+l+1), \tag{25}$$

where the above series are well defined for any n including noninteger values.

In what follows we are interested in quantities which contribute to NLO at low x, i.e., in the initial series $S_{-2}(n)$, $S_{-3}(n)$ and $S_{-2,1}(n)$, anomalous dimensions and the coefficient functions, at $n = 1 + \omega$. In the vicinity of $\omega = 0$ we have

$$S_{-2}(1+\omega) = 1 - \zeta_2 + O(\omega),$$
$$S_{-3}(1+\omega) = 1 - \frac{3}{2}\zeta_3 + O(\omega),$$
$$S_{-2,1}(1+\omega) = 1 - \frac{5}{4}\zeta_3 + O(\omega). \tag{26}$$

III. BDH-LIKE RESULTS

We reiterate that, our analysis is based on Eqs. (8) and (9) or, equivalently, on Eqs. (15), (16) and (19), where the structure function $F_2(x, Q^2)$ is supposed to be known and determined from the existing experimental data. In the present paper we employ the BDH parametrization [15], obtained from a combined fit of the H1 and ZEUS collaborations' data [27] in the following ranges of the kinematical variables x and Q^2: $x < 0.01$ and $0.15\,\mathrm{GeV}^2 < Q^2 < 3000\,\mathrm{GeV}^2$. The explicit expression for the BDH parametrization reads as

$$F_2^{\mathrm{BDH}}(x, Q^2) = D(Q^2)(1-x)^{\nu} \sum_{m=0}^{2} A_m(Q^2) L^m \tag{27}$$

where the dependence on the effective parameters is encoded in $D(Q^2)$ and $A_m(Q^2)$

$$D(Q^2) = \frac{Q^2(Q^2 + \lambda M^2)}{(Q^2 + M^2)^2},$$
$$A_0(Q^2) = a_{00} + a_{01}L_2,$$
$$A_i(Q^2) = \sum_{k=0}^{2} a_{ik}L_2^k, \quad i = (1, 2), \tag{28}$$

where the logarithmic terms L are

$$L = \ln\frac{1}{x} + L_1, \quad L_1 = \ln\left(\frac{Q^2}{Q^2 + \mu^2}\right), \quad L_2 = \ln\left(\frac{Q^2 + \mu^2}{\mu^2}\right). \tag{29}$$

The performed fit of the experimental data [27] provided the following values of the effective parameters [15]:

$$\mu^2 = 2.82 \pm 0.29\ \mathrm{GeV}^2,$$
$$M^2 = 0.753 \pm 0.008\ \mathrm{GeV}^2,$$
$$\nu = 11.49 \pm 0.99,$$
$$\lambda = 2.430 \pm 0.153, \tag{30}$$

and

$$a_{00} = 0.255 \pm 0.016, \quad a_{01} \cdot 10^1 = 1.475 \pm 0.3025,$$
$$a_{10} \cdot 10^4 = 8.205 \pm 4.620, \quad a_{11} \cdot 10^2 = -5.148 \pm 0.819,$$
$$a_{12} \cdot 10^3 = -4.725 \pm 1.010, \quad a_{20} \cdot 10^3 = 2.217 \pm 0.142,$$
$$a_{21} \cdot 10^2 = 1.244 \pm 0.0860, \quad a_{22} \cdot 10^4 = 5.958 \pm 2.320. \tag{31}$$

Notice that, the BDH parametrization (27) is written in $(x - Q^2)$ space, whereas Eq. (19) is in the space of Mellin momenta. Hence, before proceeding with a consideration of Eq. (19), we transform the BDH parametrization to Mellin space. Then, in the transformed parametrization $M_2(n, Q^2)$ we consider the first momenta $n = 1 + \omega$ and take the limit $\omega \to 0$, which corresponds to low x, and obtain

$$M_2^{\mathrm{BDH}}(n, Q^2) = D(Q^2)\sum_{m=0}^{2} A_m(Q^2)P_m(\omega, \nu, L_1) + O(\omega)$$
$$\equiv D(Q^2)\hat{M}_2^{\mathrm{BDH}}(n, Q^2), \tag{32}$$

where the quantity $P_m(\omega, \nu, L_1)$ stands for the approximate expression of the integral

$$\int_0^1 dx x^{\omega-1}(1 - x)^{\nu}L^k(x) = P_k(\omega, \nu, L_1) + O(\omega). \tag{33}$$

The explicit expression for the integral (33) is relegated to Appendix A. It should be noted that $P_k(\omega, \nu, L_1)$, besides the finite part at $\omega \to 0$, also contains negative powers of ω, i.e., it is a singular function at $\omega = 0$. These singularities are of our interests in further procedure of solving Eqs. (8)–(19). The strategy is as follows: we disregard the finite part of $M_2^{\mathrm{BDH}}(n, Q^2)$ and keep only the singular terms. Then we repeat the same procedure for the longitudinal momentum $M_L^{\mathrm{BDH}}(n, Q^2)$, Eq. (19), and equate the coefficients in front of each singularity. In such a way we obtain the representation for the longitudinal SF. Actually, in our calculations, we analyze the singularities in a slightly different way by using some specific properties of the expansions over ω, thus avoiding a direct comparison of the singular coefficients (see below). At $\omega \to 0$ the integral (33) becomes independent of ν and the singular part of $\hat{M}_2^{\mathrm{BDH}}(n, Q^2)$ can be written as

$$\hat{M}_2^{\mathrm{BDH}}(n, Q^2) = \sum_{m=0}^{2} A_m(Q^2)P_m^{\mathrm{sing}}(\omega, L_1) + O(\omega^0), \tag{34}$$

where

$$P_0^{\mathrm{sing}}(\omega) = \frac{1}{\omega}, \qquad P_1^{\mathrm{sing}}(\omega, L_1) = \frac{1}{\omega^2} + \frac{L_1}{\omega},$$
$$P_2^{\mathrm{sing}}(\omega, L_1) = \frac{2}{\omega^3} + \frac{2L_1}{\omega^2} + \frac{L_1^2}{\omega}. \tag{35}$$

Note that $P_i^{\mathrm{sing}}(\omega)$ $(i = 1, 2, 3)$ in the limit $\omega \to 0$ satisfy the following useful recurrence relations:

$$\omega P_0^{\mathrm{sing}}(\omega) = O(\omega^0),$$
$$\omega P_1^{\mathrm{sing}}(\omega) = P_0^{\mathrm{sing}}(\omega) + O(\omega^0),$$
$$\omega P_2^{\mathrm{sing}}(\omega) = 2P_1^{\mathrm{sing}}(\omega) + O(\omega^0),$$
$$\omega^2 P_2^{\mathrm{sing}}(\omega) = 2P_0^{\mathrm{sing}}(\omega) + O(\omega^0), \tag{36}$$

which are widely used subsequently.

A. Derivation of $M_2^{\mathrm{BDH}}(n,Q^2)$

To conclude the low-x analysis one needs the explicit expressions for $dM_2^{\mathrm{BDH}}(n, Q^2)/d\ln Q^2$ in Eq. (19), i.e., the derivatives of the corresponding ingredients

$$\frac{d}{d\ln Q^2}M_2^{\mathrm{BDH}}(n, Q^2) = \frac{dD(Q^2)}{d\ln Q^2}\sum_{m=0}^{2} A_m(Q^2)P_m^{\mathrm{sing}}(\omega, L_1)$$
$$+ D(Q^2)\sum_{m=0}^{2}\frac{dA_m(Q^2)}{d\ln Q^2}P_m^{\mathrm{sing}}(\omega, L_1)$$
$$+ D(Q^2)\sum_{m=0}^{2} A_m(Q^2)\frac{dP_m^{\mathrm{sing}}(\omega, L_1)}{d\ln Q^2}$$
$$+ O(\omega^0). \tag{37}$$

Noticing that

$$\frac{d}{d\ln Q^2}L_2 = \frac{Q^2}{Q^2+\mu^2},$$
$$\frac{d}{d\ln Q^2}L_1 = \frac{\mu^2}{Q^2+\mu^2},$$
$$\frac{d}{d\ln Q^2}D = \frac{M^2Q^2((2-\lambda)Q^2+\lambda M^2)}{(Q^2+M^2)^3} \equiv \tilde{D}, \quad (38)$$

we can write

$$\frac{d}{d\ln Q^2}A_m = \frac{Q^2}{Q^2+\mu^2}\bar{A}_m,$$
$$\bar{A}_m = a_{m1} + 2a_{m2}L_2,$$
$$a_{02} = 0, \quad (39)$$

$$\frac{d}{d\ln Q^2}P_m^{\rm sing}(\omega, L_1) = \frac{Q^2}{Q^2+\mu^2}\bar{P}_m^{\rm sing}(\omega, L_1),$$

$$\bar{P}_m^{\rm sing}(\omega, L_1) = (m-1)P_{m-1}^{\rm sing}(\omega, L_1). \quad (40)$$

Collecting all of the results together, we have

$$\frac{d}{d\ln Q^2}M_2^{\rm BDH}(n, Q^2) = \sum_{m=0}^{2}\hat{A}_m(Q^2)P_m^{\rm sing}(\omega, L_1) + O(\omega^0), \quad (41)$$

where

$$\hat{A}_2 = \tilde{A}_2, \quad \hat{A}_1 = \tilde{A}_1 + 2DA_2\frac{\mu^2}{Q^2+\mu^2},$$
$$\hat{A}_0 = \tilde{A}_0 + DA_1\frac{\mu^2}{Q^2+\mu^2} \quad (42)$$

and

$$\tilde{A}_i = \tilde{D}A_i + D\bar{A}_i\frac{Q^2}{Q^2+\mu^2}. \quad (43)$$

IV. LO ANALYSIS

Here we present in detail the extraction of the longitudinal SF, $F_L^{\rm BDH}(x, Q^2)$, in the LO approximation. In the LO Eq. (19) reads as

$$M_{L,\rm LO}(n, Q^2) = -2\frac{B_{L,g}^{(0)}(n)}{\gamma_{sg}^{(0)}(n)}\frac{dM_2(n, Q^2)}{d\ln Q^2} + a_s(Q^2)\tilde{B}_{L,s}^{(0)}(n)M_2(x, Q^2), \quad (44)$$

where

$$\tilde{B}_{L,s}^{(0)}(n) = B_{L,s}^{(0)}(n) - B_{L,g}^{(0)}(n)\frac{\gamma_{ss}^{(0)}(n)}{\gamma_{sg}^{(0)}(n)}. \quad (45)$$

The next step is to consider Eq. (44) at $n = 1+\omega$ and to perform the series expansion of the anomalous dimensions and the coefficient functions about $\omega = 0$. Restricting the expansion up to terms $\propto\omega^2$ we obtain

$$\frac{B_{L,g}^{(0)}(1+\omega)}{e\gamma_{sg}^{(0)}(1+\omega)} = -\frac{1}{2}\left(1+\frac{\omega}{4}-\frac{7}{16}\omega^2\right),$$
$$B_{L,s}^{(0)}(1+\omega) = 2C_F\left(1-\frac{\omega}{2}+\frac{\omega^2}{4}\right),$$
$$\gamma_{ss}^{(0)}(1+\omega) = 8C_F\omega\left(\zeta(2)-\frac{5}{8}+\left(\frac{9}{16}-\zeta(3)\right)\omega\right). \quad (46)$$

Observe that, in the above Eq. (44) both, the momentum $M_2(x, Q^2)$ and the derivative $dM_2(n, Q^2)/d\ln Q^2$ are of a similar form, cf. Eqs. (34) and (41), so that the rhs of Eq. (44) with the expansions (46) can be represented as

$$\sum_{m=0}^{2}A_mP_m^{\rm sing} \times (\text{a cubic polynomial in } \omega).$$

This substantially simplifies the calculations since, in such a case, we can apply the recurrence relations (36) to find the desired coefficients. For instance, for any (known) series of the form

$$T(\omega) = T_0 + T_1\omega + T_2\omega^2 + O(\omega^3) \quad (47)$$

one easily obtains the result

$$T(\omega)\sum_{m=0}^{2}A_mP_m^{\rm sing} = T_0\sum_{m=0}^{2}A_mP_m^{\rm sing} + T_1(2A_2P_2^{\rm sing} + A_1P_1^{\rm sing}) + 2T_2A_2P_1^{\rm sing} + O(\omega^0)$$
$$= \sum_{m=0}^{2}\bar{\bar{A}}_mP_m^{\rm sing} + O(\omega^0), \quad (48)$$

where

$$\bar{\bar{A}}_2 = T_0A_2,$$
$$\bar{\bar{A}}_1 = T_0A_1 + 2T_1A_2,$$
$$\bar{\bar{A}}_0 = T_0A_0 + T_1A_1 + 2T_2A_2. \quad (49)$$

It is seen that it is sufficient to determine the coefficients T_0, T_1 and T_2 to find the solution of the system, avoiding in such a way, lengthy and cumbersome calculations. In our case the explicit expressions for T_i can be inferred directly from Eq. (46). Then the coefficients C_m of the LO expansions of the longitudinal Mellin momenta

$$M_{L,\mathrm{LO}}^{\mathrm{BDH}}(n,Q^2)=\sum_{m=0}^{2}C_m P_m^{\mathrm{sing}}+O(\omega^0), \qquad (50)$$

explicitly read as

$$\begin{aligned}C_2&=\hat{A}_2+\frac{8}{3}a_s D A_2,\\ C_1&=\hat{A}_1+\frac{1}{2}\hat{A}_2+\frac{8}{3}a_s D\left(A_1+\left(4\zeta_2-\frac{7}{2}\right)A_2\right),\\ C_0&=\hat{A}_0+\frac{1}{4}\hat{A}_2-\frac{7}{8}\hat{A}_2+\frac{8}{3}a_s D\left(A_0+\left(2\zeta_2-\frac{7}{4}\right)A_1\right.\\ &\quad\left.+\left(\zeta_2-4\zeta_3+\frac{17}{8}\right)A_2\right). \qquad (51)\end{aligned}$$

It is worth mentioning once more that, the above results for C_i ($i=0,1,2$) have been obtained in a straightforward way by avoiding direct comparisons of singularities in Eq. (44), as previously reported in Refs. [26,37]. Another important result is that the adopted BDH parametrization for $F_2(x,Q^2)$ led directly to the same BDH-like form of the longitudinal structure functions $F_{L,\mathrm{LO}}^{\mathrm{BDH}}(x,Q^2)$ which, consequently, also obey the Froissart boundary condition

$$F_{L,\mathrm{LO}}^{\mathrm{BDH}}(x,Q^2)=(1-x)^{\nu_L}\sum_{m=0}^{2}C_m(Q^2)L^m, \qquad (52)$$

where, for simplicity, we adopt $\nu_L=\nu$. In principle, at large x the quark counting rules [43] predict a rather different behaviour of the valence and sea quark distributions. Since we consider the small-x kinematics, our choice of ν_L does not affect the analysis.

V. NLO ANALYSIS

In this section we discuss the longitudinal structure function within the NLO approximation. As before, particular attention is paid to the region of asymptotically small $x\to 0$ in the context of the Froissart boundary.

Multiplying both sides of Eq. (19) by the factor $(1+a_s(Q^2)[\delta_{sg}^{(1)}(n)-R_{L,g}^{(1)}(n)])$, we have

$$\begin{aligned}&(1+a_s(Q^2)[\delta_{sg}^{(1)}(n)-R_{L,g}^{(1)}(n)])M_L(n,Q^2)\\ &\quad=-2\frac{B_{L,g}^{(0)}(n)}{\gamma_{sg}^{(0)}(n)}\frac{dM_2(n,Q^2)}{d\ln Q^2}+a_s(Q^2)(\tilde{B}_{L,s}^{(0)}(n)\\ &\qquad+a_s(Q^2)\tilde{B}_{L,s}^{(1)}(n))M_2(n,Q^2)+O(a_s^3), \qquad (53)\end{aligned}$$

where

$$\delta_{sa}^{(1)}(n)=\frac{\tilde{\gamma}_{sa}^{(1)}(n)}{\gamma_{sg}^{(0)}(n)}, \qquad R_{L,a}^{(1)}(n)=\frac{\tilde{B}_{L,a}^{(1)}(n)}{B_{L,a}^{(0)}(n)} \qquad (54)$$

and

$$\begin{aligned}\tilde{B}_{L,s}^{(1)}(n)&=B_{L,s}^{(0)}(n)(R_{L,s}^{(1)}(n)+\delta_{sg}^{(1)}(n)-R_{L,g}^{(1)}(n))\\ &\quad-B_{L,g}^{(0)}(n)\delta_{ss}^{(1)}(n). \qquad (55)\end{aligned}$$

Using Eqs. (44) and (53) together, it is straightforward to obtain

$$\begin{aligned}&(1+a_s(Q^2)[\delta_{sg}^{(1)}(n)-R_{L,g}^{(1)}(n)])M_L(n,Q^2)\\ &\quad=M_{L,\mathrm{LO}}(n,Q^2)+a_s^2(Q^2)\tilde{B}_{L,s}^{(1)}(n)M_2(n,Q^2). \qquad (56)\end{aligned}$$

When computing the inverse Mellin transform of Eq. (56) we use the fact that on the lhs of Eq. (56), up to $O(a_s^3)$ corrections, we can write

$$\begin{aligned}&a_s(Q^2)[\delta_{sg}^{(1)}(n)-R_{L,g}^{(1)}(n)]M_L(n,Q^2)\\ &\quad=a_s(Q^2)[\delta_{sg}^{(1)}(n)-R_{L,g}^{(1)}(n)]M_{L,\mathrm{LO}}(n,Q^2)+O(a_s^3), \qquad (57)\end{aligned}$$

where the LO momentum $M_{L,\mathrm{LO}}(n,Q^2)$ has already been calculated in the previous section, cf. Eq. (50).

Prior to proceeding with the inverse Mellin transforms, it is convenient to extract the singular structure of the NLO coefficients $\delta_{sg}^{(1)}(n)$, $R_{L,g}^{(1)}(n)$ and $\tilde{B}_{L,s}^{(1)}(n)$. We have

$$\begin{aligned}\delta_{sg}^{(1)}(n)&=\frac{\hat{\delta}_{sa}^{(1)}}{\omega}+\bar{\delta}_{sa}^{(1)}(1+\omega),\\ R_{L,g}^{(1)}(n)&=\frac{\hat{R}_{L,g}^{(1)}}{\omega}+\bar{R}_{L,g}^{(1)}(1+\omega),\\ \tilde{B}_{L,s}^{(1)}(n)&=\frac{\hat{B}_{L,g}^{(1)}}{\omega}+\bar{B}_{L,g}^{(1)}(1+\omega), \qquad (58)\end{aligned}$$

with ($\omega\to 0$)

$$\begin{aligned}\hat{B}_{L,s}^{(1)}&=\frac{20}{3}C_F(3C_A-2f),\\ \bar{B}_{L,s}^{(1)}(1)&=8C_F\left[\frac{25}{9}f-\frac{449}{72}C_F\right.\\ &\quad\left.+(2C_F-C_A)\left(\zeta_3+2\zeta_2-\frac{59}{72}\right)\right],\\ \hat{\delta}_{sg}^{(1)}&=\frac{26}{3}C_A, \qquad \bar{\delta}_{sg}^{(1)}(1)=3C_F-\frac{347}{18}C_A,\\ \hat{R}_{L,g}^{(1)}&=-\frac{4}{3}C_A, \qquad \bar{R}_{L,g}^{(1)}(1)=-5C_F-\frac{4}{9}C_A. \qquad (59)\end{aligned}$$

Then, Eq. (56) can be rewritten in the following form:

$$M_L(n,Q^2)+\frac{a_s(Q^2)}{\omega}[\hat{\delta}_{sg}^{(1)}(n)-\hat{R}_{L,g}^{(1)}(n)]M_{L,\mathrm{LO}}(n,Q^2)$$
$$=(1-a_s(Q^2)[\bar{\delta}_{sg}^{(1)}(n)-\bar{R}_{L,g}^{(1)}(n)])$$
$$\times M_{L,\mathrm{LO}}(n,Q^2)+a_s^2(Q^2)\left[\frac{\hat{B}_{L,s}^{(1)}}{\omega}+\bar{B}_{L,s}^{(1)}(n)\right]$$
$$\times M_2(n,Q^2)+O(a_s^3). \tag{60}$$

Now the inverse Mellin transforms of the last equations can be easily performed (see also Appendix B). The result is

$$F_L^{\mathrm{BDH}}(x,Q^2)+\frac{a_s(Q^2)}{3}L_C[\hat{\delta}_{sg}^{(1)}-\hat{R}_{L,g}^{(1)}]F_{L,\mathrm{LO}}^{\mathrm{BDH}}(x,Q^2)$$
$$=[1-a_s(Q^2)(\bar{\delta}_{sg}^{(1)}(1)-\bar{R}_{L,g}^{(1)}(1))]F_{L,\mathrm{LO}}^{\mathrm{BDH}}(x,Q^2)$$
$$-a_s^2(Q^2)\left[\frac{\hat{B}_{L,s}^{(1)}}{3}L_A+\bar{B}_{L,s}^{(1)}(1)\right]M_2^{\mathrm{BDH}}(x,Q^2), \tag{61}$$

where

$$L_A=L+\frac{A_1}{2A_2},\qquad L_C=L+\frac{C_1}{2C_2}. \tag{62}$$

With the considered accuracy the obtained equation (61) can be rewritten as

$$\left[1+\frac{1}{3}a_s(Q^2)L_C(\hat{\delta}_{sg}^{(1)}-\hat{R}_{L,g}^{(1)})\right]F_L^{\mathrm{BDH}}(x,Q^2)$$
$$=[1-a_s(Q^2)(\bar{\delta}_{sg}^{(1)}-\bar{R}_{L,g})]F_{L,\mathrm{LO}}^{\mathrm{BDH}}(x,Q^2)$$
$$-a_s^2(Q^2)\left[\frac{1}{3}\hat{B}_{L,s}^{(1)}L_A+\bar{B}_{L,s}^{(1)}(1)\right]M_2^{\mathrm{BDH}}(x,Q^2)$$
$$+O(a_s^3). \tag{63}$$

Eventually, the final expression for the longitudinal SF $\hat{F}_L^{\mathrm{BDH}}(x,Q^2)$ reads as

$$F_L^{\mathrm{BDH}}(x,Q^2)=\frac{1}{[1+\frac{1}{3}a_s(Q^2)L_C(\hat{\delta}_{sg}^{(1)}(1)-\hat{R}_{L,g}^{(1)})]}$$
$$\times\left\{[1-a_s(Q^2)(\bar{\delta}_{sg}^{(1)}-\bar{R}_{L,g})]F_{L,\mathrm{LO}}^{\mathrm{BDH}}(x,Q^2)\right.$$
$$-a_s^2(Q^2)\left[\frac{1}{3}\hat{B}_{L,s}^{(1)}L_A+\bar{B}_{L,s}^{(1)}(1)\right]$$
$$\left.\times F_2^{\mathrm{BDH}}(x,Q^2)\right\}. \tag{64}$$

This is our final expression for the longitudinal SF $F_L^{\mathrm{BDH}}(x,Q^2)$ within the NLO approximation for low values of x.

VI. RESULTS

With the explicit form of the basic expressions described above, we can proceed to extract the longitudinal structure function $F_L(x,Q^2)$ from data described by the BDH parametrization of $F_2^{\mathrm{BDH}}(x,Q^2)$. In our calculations we employ the standard representation for QCD couplings in the LO and NLO (within the $\overline{\mathrm{MS}}$ scheme) approximations

$$a_s(Q^2)=\frac{1}{\beta_0\ln(Q^2/\Lambda^2)}\ \ (\mathrm{LO}),$$
$$a_s(Q^2)=\frac{1}{\beta_0\ln(Q^2/\Lambda^2)}-\frac{\beta_1\ln\ln(Q^2/\Lambda^2)}{\beta_0[\beta_0\ln(Q^2/\Lambda^2)]^2}\ \ (\mathrm{NLO}). \tag{65}$$

The QCD parameter Λ has been extracted from the running coupling α_s normalized at the Z-boson mass, $\alpha_s(M_Z^2)$, using the b- and c-quark thresholds according to Ref. [44]. Applying this procedure to ZEUS data, with $\alpha_s(M_Z^2)=0.1166$ [45], we obtain the following results for Λ, cf. Ref. [46]:

$$\begin{aligned}\mathrm{LO}:\ &\Lambda(f=5)=80.80\ \mathrm{MeV},\\ &\Lambda(f=4)=136.8\ \mathrm{MeV},\\ &\Lambda(f=3)=136.8\ \mathrm{MeV},\\ \mathrm{NLO}:\ &\Lambda(f=5)=195.7\ \mathrm{MeV},\\ &\Lambda(f=4)=284.0\ \mathrm{MeV},\\ &\Lambda(f=3)=347.2\ \mathrm{MeV}.\end{aligned} \tag{66}$$

We have calculated the Q^2 dependence, at low x, of the longitudinal structure function $F_L^{\mathrm{BDH}}(x,Q^2)$ as described above, in the LO [Eq. (52)] and NLO [Eq. (64)] approximations. The results of our calculations and a comparison with data from the H1 Collaboration [47] are presented in Fig. 1, where the dashed and solid lines correspond to the extracted SF in the LO and NLO approximations, respectively. Calculations have been performed at a fixed value of the invariant mass W, $W=230$ GeV, allowing the Bjorken variable x to vary in the interval $(3\times10^{-5}<x<7\times10^{-2})$ when Q^2 varies in the interval $(1\ \mathrm{GeV}^2<Q^2<3000\ \mathrm{GeV}^2)$. Figure 1 clearly demonstrates that the extraction procedure provides the correct behaviors of the extracted SF in both the LO and NLO approximations. At intermediate and high Q^2 the extracted SFs are in good agreement with experimental data. In this region the NLO corrections are rather small and can be neglected. A different situation occurs at low $Q^2<5\ \mathrm{GeV}^2$, where the LO $F_L(x,Q^2)$ substantially exceeds experimental data. The NLO corrections here are negative and result in a better agreement with data. However, at extremely low momenta, $Q^2<1.5\ \mathrm{GeV}^2$, the extracted SF within NLO is still above the experimental data. It should also be mentioned that our calculations are consistent with other theoretical results, obtained, e.g., in the framework of

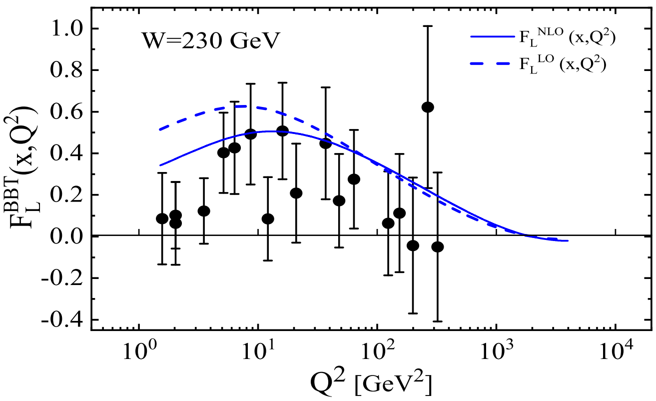

FIG. 1. The extracted longitudinal structure function $F_L(x, Q^2)$ from the BDH parametrization of $F_2(x, Q^2)$ at a fixed value of the invariant mass $W = 230$ GeV. The dashed line represents calculations within the LO approximation [Eq. (52)], while the solid line represents the structure function within the NLO approximation [Eq. (64)]. Experimental data are from the H1 Collaboration [47]. The Bjorken variable x corresponding to the chosen kinematics lies in the interval $(3 \times 10^{-5} < x < 7 \times 10^{-2})$.

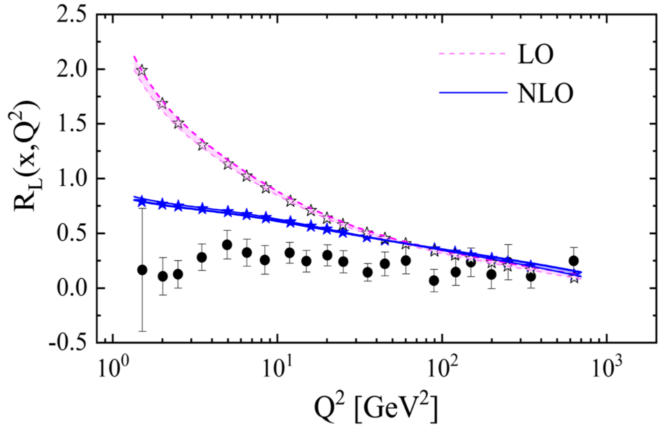

FIG. 2. The ratio of the longitudinal to transversal cross sections, Eq. (67), calculated with the extracted longitudinal SF within the leading- and next-to-leading-order approximations. The open and full stars are the results of LO and NLO calculations, respectively, within the exact kinematical conditions reported in Ref. [47], i.e., for each experimental point the variable x is taken from the corresponding (Q^2, x) bin. The shaded areas are calculations with minimal and maximal values of W from Table 6 of Ref. [47]: $W = 232$ GeV and $W = 184$ GeV for the upper and lower boundaries, respectively.

perturbation theory [7,8] and/or in Ref. [48] in the so-called k_t-factorization approach [49], both of which incorporate the BFKL resummation [10] at low x (for a review of low-x phenomenology see, e.g., Ref. [50]). Recall that the inclusion of the BFKL resummation in a study of PDFs leads to an improvement of the description of data at small x and nowadays appears as an integral part in a majority of approaches. The NNPDF Collaboration [51] and the xFITTER HERAPDF team [27,52], whose approaches are based on the DGLAP equations, recently included the BFKL resummation in their analysis of the combined H1 + ZEUS inclusive cross section [53] achieving, in such a way, a much better description of the data [7,8]. Analogous studies have been performed in Refs. [7,54–56]. This is in some contrast to the results of the standard PDF sets [4,6,51,52] without the BFKL resummations.

A particular interests presents the ratio of the longitudinal to transversal cross sections, defined as

$$R_L(x, Q^2) = \frac{F_L(x, Q^2)}{F_2(x, Q^2) - F_L(x, Q^2)}. \tag{67}$$

Recently, the H1 Collaboration reported the ratio $R_L(x, Q^2)$ measured in several kinematical bins of averaged Q^2 and x, cf. Table 6 of Ref. [47]. Within such kinematics, the invariant mass W changes from $W \sim 230$ GeV to $W \sim 184$ GeV with an increase of Q^2 and x in the selected bins. In Fig. 2 we present the ratio (67), calculated with the extracted $F_L^{\rm BDH}(x, Q^2)$ and parametrized $F_2^{\rm BDH}(x, Q^2)$, in comparison with the mentioned H1 data. The open and full stars are the results of calculations within the LO and NLO approximations, where x and Q^2 correspond exactly to the experimental bins reported in Ref. [47]. The shaded areas are calculations for two fixed (minimal and maximal) values of the invariant mass W within the chosen bins. From Fig. 2 one can infer that the NLO results essentially improve the agreement with the data in comparison with the LO calculations. As in the previous case, the extracted longitudinal SF $F_L^{\rm BDH}(x, Q^2)$ slightly overestimates the data at relatively low Q^2.

Now we proceed with an analysis of the x evolution of the longitudinal SF at fixed Q^2. As mentioned above, the investigation of $F_L(x, Q^2)$ as a function of x is of interest in connection with theoretical investigations of ultrahigh-energy processes with cosmic neutrinos and also in the context of the Froissart restrictions at $x \to 0$. We have calculated the x dependence of the longitudinal SF at several fixed values of Q^2 corresponding to H1 Collaboration data. The results are presented in Fig. 3 where the x evolution of $F_L(x, Q^2)$ is clearly exhibited. It is seen that, for all values of the presented Q^2, the extracted SF within the NLO approximation is in much better agreement with the data. This persuades us that the obtained SF in the NLO approximation can be pertinent in future analyses of ultrahigh-energy neutrino data.

In Fig. 4 we present the ratio (67) calculated for the same kinematics as in Fig. 3. As in previous calculations, the NLO results are in better agreement with the data. It is also seen from Fig. 4 that the NLO ratio $R_L(x, Q^2)$ exhibits a tendency to be almost independent on x in each bin of Q^2, decreasing, however, as Q^2 increases, as it should be. We also mention that, as in the case of Q^2 dependence, our extracted longitudinal SF as a function of x is in reasonably

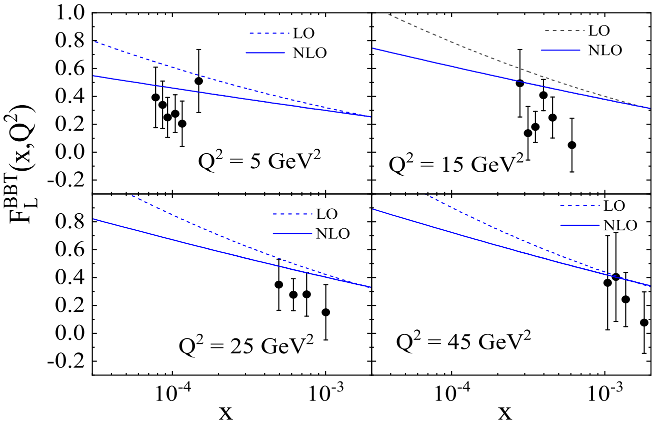

FIG. 3. The longitudinal structure function $F_L(x, Q^2)$ extracted from the BDH parametrization of $F_2(x, Q^2)$ at fixed Q^2 as a function of the Bjorken variable x. The dashed lines represent results of calculations within the LO approximation, while the solid lines represent the SFs obtained within the NLO approximation. Experimental data are from the H1 Collaboration [47].

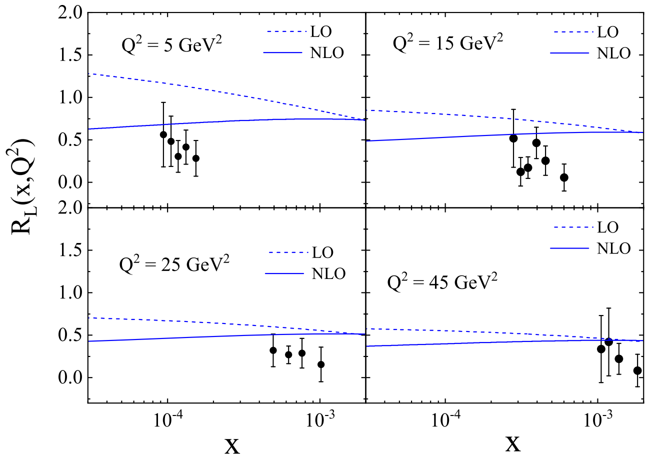

FIG. 4. The same as in Fig. 3, but for the ratio of the longitudinal to transversal cross sections, $R_L(x, Q^2)$, Eq. (67).

good agreement with other theoretical predictions; see e.g., Refs. [7,8] for pQCD results and/or Ref. [57] for results obtained within the k_t-factorization approach. Likewise our results are in good agreement with the previous investigations reported in Ref. [23], where a similar analysis has been performed within the framework of pQCD, with the experimental data for the transverse SF $F_2(x, Q^2)$ and the logarithmic derivative $dF_2/d\ln(Q^2)$.

VII. CONCLUSIONS AND OUTLOOK

In this paper, we presented a further development of the method of extracting the longitudinal DIS structure function $F_L(x, Q^2)$ suggested in Refs. [22,23,26]. The method relies on the DGLAP equations and on the Froissart-bounded parametrization of the DIS structure function $F_2(x, Q^2)$. We focused our attention on the kinematical region of low Bjorken variable ($10^{-5} \lesssim x \lesssim 0.1$) in a large interval of the momentum transfer (1 GeV$^2 \lesssim Q^2 \lesssim 3 \times 10^3$ GeV^2). The extraction procedure has been elaborated for an analysis of the SF $F_L(x, Q^2)$ within the leading- and next-to-leading-order approximations. To this end, we considered the known transversal SF $F_2(x, Q^2)$ and used the DGLAP equations to relate it to the longitudinal SF. Then, in the space of Mellin momenta we found, up to α_s^2 corrections, the corresponding Mellin transforms for the momenta corresponding to low and ultralow values of x. The inverse Mellin transform provides the desired longitudinal SF in the usual $x - Q^2$ representation. The obtained explicit expression for $F_L(x, Q^2)$ is entirely determined by the effective parameters of the BDH parametrization (27) and is presented in Eq. (64). Some comments are in order here. Observe that, the final expression (64) contains the dominant logarithmic terms $\sim\ln(1/x)$ in both the numerator and denominator. In principle, due to the smallness of the running coupling $\alpha_s(x, Q^2)$, the denominator with L_C can be rewritten in the numerator as an alternate series leading to a behavior similar to the one known within pQCD, where the NLO corrections, in the considered kinematical region, are negative and large, while NNLO contributions are positive and also large (see, e.g., Ref. [58]). A resummation of these contributions would allow to avoid such an alternate behavior. In our case, this is achieved by keeping the logarithmic term in the denominator without expanding it into series relative to $\alpha_s(x, Q^2)$. To some extent, our representation of the basic NLO corrections, Eq. (64), can be considered as an effective resummation of the most important (at low x) logarithmic terms in each order of the perturbation theory. Another observation is that by keeping the logarithmic L_C terms in the denominator we also manifestly demonstrate that the SF $F_L(x, Q^2)$ obeys the Froissart conditions. As shown in Appendix B, the logarithmic part in Eq. (64) is a direct consequence of the inverse Mellin transforms of terms $\sim 1/\omega$.

We have applied the developed method to extract the longitudinal SF within kinematical conditions corresponding to those available at the HERA collider. It has been found that, at relatively large $Q^2 > 10$ GeV^2 both, LO and NLO results reproduce fairly well the experimental data. At smaller Q^2 the LO approximation fails to describe the data, being systematically larger. Accounting for NLO corrections, which at low x turn out to be negative, substantially improves the description of the SF and the ratio of the longitudinal to transversal cross section. However, at extremely low momentum transfer $Q^2 \lesssim 1$ GeV^2, the extracted SF still exceeds the data.

We have performed an analysis of the x evolution of the extracted SF. It has been demonstrated that the x dependence of $F_L(x, Q^2)$ also reproduces the behavior of the experimental data at low x. Both, the extracted SF and the ratio $R_L(x, Q^2)$ as functions of x, are in fairly good agreement with the data, while the NLO results are in much better agreement not only with the data, but also with other existing theoretical investigations based on perturbative QCD, improved by the BFKL resummation (see Refs. [7,8] and references therein), as well as with the results [48] obtained in the framework of the k_t-factorization method [49], also based on the BFKL approach [10]. Calculations of the longitudinal SF based on traditional pQCD without such improvements turn out to be rather unstable, due to the fact that the subsequent perturbative corrections can be even larger than the previous ones [58,59]. The incorporation of corrections inspired by the BFKL resummation leads to substantially more stable results for $F_L(x, Q^2)$ [59] (see also similar investigations in Refs. [7,54–56]), and allows to achieve a rather good description of the combined H1 + ZEUS inclusive cross sections [53].

Apart from the study of the Froissart boundary restrictions, the knowledge of the $F_L(x, Q^2)$ at low x is of great interest in connection with the theoretical treatments of the ultrahigh-energy processes with cosmic neutrinos. As already mentioned in the Introduction, the NLO approximation for $F_L(x, Q^2)$, i.e., calculations up to α_s^2 corrections, corresponds to the NNLO for $F_2(x, Q^2)$ which, in the LO, is $\propto \alpha_s^0$. Consequently, with the NLO results (64), in our approach it becomes possible to perform NLO and NNLO analyses of the ultrahigh-energy ($\sqrt{s} \sim 1$ TeV) neutrino cross sections similar to NLO [29] and NNLO [30] investigations based on pQCD. Such calculations are of great importance in view of expected reliable cross sections from existing and forthcoming data at IceCube [32] and from the substantially improved IceCube-Gen2 [33]. Therefore, a direct comparison of the theoretical predictions with experimental data becomes feasible.

In the kinematical region where the gluon contributions are sizable the (large) corrections within traditional pQCD can be strongly reduced by a proper change of the factorization and renormalization scales [60]. An analysis of the precise H1 + ZEUS combined data [27] obtained within the kinematics near the limit of applicability of pQCD has shown [61] that using effective scales with large parameters provides much smaller high-order perturbative corrections. In such a case the strong couplings decrease as well and, as a rule, calculations with effective scales lead to better agreement with data [cf. investigations of the NLO corrections in the context of high-energy asymptotics of virtual photon-photon collisions [62] and studies of $F_L(x, Q^2)$ in the framework of the k_t-fragmentation approach [48]]. This encourages us to continue our low-x analysis of the SFs by implementing a special change in the factorization and renormalization scales [60]. This is the subject of our further investigations and results will be presented elsewhere.

Furthermore, we plan to improve our approach by modifying the method to extract, in the LO and NLO approximations, the gluon densities as well. We shall note that, the gluon distribution is by far less known, both experimentally and theoretically. Even the shape of the gluon density is often taken to be quite different in different PDF sets [6,9], although considered within the same framework of pQCD. However, the range of variation of the gluon density strongly decreases when BFKL resummation is included in the analyses at low x (see the most recent publication [30] and the discussion therein).

An extraction of the gluon distributions from experimental data, performed within an approach similar to the one suggested in the present paper, can provide valuable additional information on the problem. Such an analysis can be accomplished by employing the charm, $F_2^{cc}(x, Q^2)$, and beauty, $F_2^{bb}(x, Q^2)$, components of the SF $F_2(x, Q^2)$, which are directly related to the gluon density in photogluon fusion reactions (see Ref. [63] and the discussion therein). The extracted SFs can be compared with the recently obtained combined H1 + ZEUS data [64] for $F_2^{cc}(x, Q^2)$ and $F_2^{bb}(x, Q^2)$ and with the theoretical predictions [30] based on pQCD with BFKL corrections included, and also with the results [65] obtained in the framework of k_t fragmentation.

Furthermore, the charmed parts of the transverse SF $F_2^{cc}(x, Q^2)$ and longitudinal SF $F_L^{cc}(x, Q^2)$ calculated within our approach, can be used to predict the charmed part of the neutrino-nucleon cross sections at ultrahigh energy and to compare with other calculations [30] based on pQCD with BFKL corrections. Yet, the BDH gluon density itself can serve as a useful tool for estimations of the cross sections with cosmic rays, cf. Ref. [66] (for a more recent review on the subject, see Ref. [67] and references therein). Recall that, the gluon density in the BDH-like form already contains information about the violation of the standard DGLAP evolution (cf. discussions in Sec. II) and indicates the possible presence of shadowing effects, which are among the basic subjects of physical programs of operating (e.g., NICA in Dubna) and planned facilities (EIC@China, ELIC@JLAB, ENC@GSI, etc.) aimed at studying the properties of nuclear matter at high energies [68]. Our investigations in this direction are in progress.

In summary, we presented a theoretical method to extract, from the experimental data, the longitudinal DIS structure function $F_L(x, Q^2)$ at low x within the leading- and next-to-leading-order approximations. Explicit, analytical expressions for the structure function in both the LO and NLO approximations have been obtained in terms of the effective parameters of the Froissart-bound parametrization of $F_2(x, Q^2)$ and the results of numerical calculations as well as comparisons with available experimental were presented.

ACKNOWLEDGMENTS

Support by the National Natural Science Foundation of China (Grant No. 11575254) and the National Key

Research and Development Program of China (No. 2016YFE0130800) is acknowledged. L. P. K. and A. V. K. greatly appreciate the warm hospitality at the Institute of Modern Physics and thank the CAS President's International Fellowship Initiative (Grants No. 2018VMA0029 and No. 2017VMA0040) for support.

APPENDIX A: DETAILS OF THE EVALUATION OF SOME RELEVANT INTEGRALS

Here we present the evaluation of the integrals $P_k(\omega,\nu)$ $(k=0,1,2)$ appearing in Eq. (33). They can be rewritten in a more general form

$$\hat{P}_k(\omega,\nu) = \int_0^1 dx x^{\omega-1}(1-x)^{\nu}\left(\ln\frac{1}{x}\right)^k = \left(-\frac{d}{d\omega}\right)^k \int_0^1 dx x^{\omega-1}(1-x)^{\nu}, \quad (k=0,1,2). \tag{A1}$$

1. $k=0$

$$\hat{P}_0(\omega,\nu) = \int_0^1 dx x^{\omega-1}(1-x)^{\nu} = \frac{\Gamma(\omega)\Gamma(\nu+1)}{\Gamma(\omega+\nu+1)} = \frac{1}{\omega}\frac{\Gamma(\omega+1)\Gamma(\nu+1)}{\Gamma(\omega+\nu+1)}. \tag{A2}$$

The last results on the rhs can be represented as (cf. also Ref. [69])

$$\frac{\Gamma(\omega+1)\Gamma(\nu+1)}{\Gamma(\omega+\nu+1)} = \exp\left[-\sum_{i=1}^{\infty} S_i(\nu)\omega^i\right], \tag{A3}$$

where the nested sums $S_i(\nu)$ are defined by Eqs. (24) and (25).

Expanding the rhs of Eq. (A2) in ω series, we have

$$\hat{P}_0(\omega,\nu) = \frac{1}{\omega} - S_1(\nu). \tag{A4}$$

2. $k=1, 2$

For the next basic integral $\hat{P}_1(\omega)$ we have

$$\hat{P}_1(\omega,\nu) = \left(-\frac{d}{d\omega}\right) \hat{P}_0(\omega,\nu) = \left(-\frac{d}{d\omega}\right)\frac{1}{\omega}\frac{\Gamma(\omega+1)\Gamma(\nu+1)}{\Gamma(\omega+\nu+1)}. \tag{A5}$$

Expanding the rhs of Eq. (A5) in series with respect to ω, we have

$$\hat{P}_1(\omega,\nu) = \frac{1}{\omega^2} - Z_2(\nu), \tag{A6}$$

where (see, for example, Ref. [70])

$$Z_1(\nu) = S_1(\nu),$$
$$Z_2(\nu) = \frac{1}{2}S_1^2(\nu) - \frac{1}{2}S_2(\nu),$$
$$Z_3(\nu) = \frac{1}{6}S_1^2(\nu) - \frac{1}{2}S_1(\nu)S_2(\nu) + S_3(\nu), \tag{A7}$$

where $S_i(\nu)$, for integer ν, are the known harmonic numbers $S_i(\nu) = \sum_{k=1}^{\nu} 1/k^i$. For arbitrary arguments ν, these coefficients are related to the Euler $\Psi(1+\nu)$ function and its derivatives $\Psi^{(m)}(1+\nu) = d/(d\nu)\Psi(1+\nu)$ as

$$S_1(\nu) = \Psi(1+\nu) + \gamma_{\rm E},$$
$$S_2(\nu) = \zeta_2 - \Psi^{(1)}(1+\nu),$$
$$S_2(\nu) = \frac{1}{2}(\Psi^{(2)}(1+\nu) - \zeta_3), \tag{A8}$$

where $\gamma_{\rm E}$ is the Euler constant and ζ_i are Euler ζ functions.

Analogous calculations for $\hat{P}_2(\omega)$ provide

$$\hat{P}_2(\omega,\nu) = \left(-\frac{d}{d\omega}\right)^2 \hat{P}_0(\omega,\nu) = \left(-\frac{d}{d\omega}\right)^2 \frac{1}{\omega}\frac{\Gamma(\omega+1)\Gamma(\nu+1)}{\Gamma(\omega+\nu+1)}, \tag{A9}$$

which, being expanded in series about ω, results in

$$\hat{P}_2(\omega,\nu) = 2\left(\frac{1}{\omega^3} - Z_3(\nu)\right). \tag{A10}$$

Equations (A4), (A6) and (A10) allow to write the considered integral (34) as

$$\int_0^1 dx x^{\omega-1}(1-x)^{\nu}L^k(x) = P_k(\omega,\nu) + O(\omega), \tag{A11}$$

where

$$P_0(\omega,\nu) = \frac{1}{\omega} - Z_1(\nu),$$
$$P_1(\omega,\nu,L_1) = \frac{1}{\omega^2} - Z_2(\nu) + L_1 P_0(\omega,\nu),$$
$$P_2(\omega,\nu,L_1) = 2\left(\frac{1}{\omega^3} - Z_3(\nu)\right) + 2L_1 P_1(\omega,\nu) + L_1^2 P_0(\omega,\nu). \tag{A12}$$

In Eq. (A12) the finite part of the integral is encoded in the functions $Z(\nu)$ [Eq. (A7)], while the singular one is given by Eq. (35).

3. $k = 3$

Consider now the integral

$$\int_0^1 dx x^{\omega-1}(1-x)^\nu \left(\ln\frac{1}{x}\right)^3 = P_3(\omega,\nu) + O(\omega), \qquad \text{(A13)}$$

which is the third derivative of $\hat{P}_3(\omega)$ with respect to ω

$$\hat{P}_3(\omega,\nu) = \left(-\frac{d}{d\omega}\right)^3 \hat{P}_0(\omega,\nu) = \left(-\frac{d}{d\omega}\right)^2 \frac{1}{\omega}\frac{\Gamma(\omega+1)\Gamma(\nu+1)}{\Gamma(\omega+\nu+1)}. \qquad \text{(A14)}$$

Eventually, at $\omega \to 0$ we obtain

$$\hat{P}_3(\omega,\nu) = 6\left(\frac{1}{\omega^4} + O(\omega^0)\right). \qquad \text{(A15)}$$

APPENDIX B: INVERSE MELLIN TRANSFORMS AT LOW x

In this Appendix we present some details of the calculation of the inverse Mellin transform of the longitudinal momentum $M_L(n,Q^2)$, Eq. (56). Observe, that $M_L(n,Q^2)$ is expressed via $M_L^{LO}(n,Q^2)$ and $M_2^{\rm BDH}(n,Q^2)$. Hence, it is sufficient to determine the inverse Mellin transforms of $M_2^{\rm BDH}(n,Q^2)$ augmented with some coefficients depending on ω to find the desired longitudinal SF $F_L(x,Q^2)$. To facilitate the calculations, consider the following auxiliary integral:

$$I(\omega,Q^2) = \int_0^1 dx x^{\omega-1}\left(\ln\frac{1}{x}\right) F_2^{\rm BDH}(x,Q^2). \qquad \text{(B1)}$$

It is obvious that this integral is proportional to the Mellin transform $M_2(\omega,Q^2)$ with some coefficients of proportionality as functions of ω,

$$I(\omega,Q^2) \propto \left(\frac{K_{-1}}{\omega} + K_0 + K_1\omega + K_2\omega^2 + \cdots\right) M_2^{\rm BDH}(\omega,Q^2). \qquad \text{(B2)}$$

If so, we can avoid the direct calculation of the inverse Mellin transform of $M_2^{\rm BDH}(\omega,Q^2)$. Instead, for any constants $\hat{F}_1$ and $\hat{F}_2$ and vanishing ω, we can use the obvious relation

$$\left(\frac{\hat{F}_1}{\omega} + \hat{F}_2\right) M_2^{\rm BDH}(\omega,Q^2) \xrightarrow{\text{Inverse Mellin}} \left(\frac{\hat{F}_1}{3}L_A + \hat{F}_2\right) F_2^{\rm BDH}(x,Q^2), \qquad \text{(B3)}$$

where $L_A = \ln\frac{1}{x} + L_1 + \frac{A_1}{2A_2}$, cf. Eqs. (62) and (29). The integral $I(\omega,Q^2)$ in Eq. (B1) can be calculated directly by using Eqs. (A4), (A6), (A10) and (A15). Up to $\mathcal{O}(\omega^0)$, we have

$$\int_0^1 dx x^{\omega-1}\left(\ln\frac{1}{x}\right) F_2^{\rm BDH}(x,Q^2) = D\left[A_0\frac{1}{\omega^2} + A_1\left(\frac{2}{\omega^3} + \frac{L_1}{\omega^2}\right) + A_2\left(\frac{6}{\omega^4} + \frac{4L_1}{\omega^3} + \frac{L_1^2}{\omega^2}\right)\right]. \qquad \text{(B4)}$$

Inserting Eqs. (32), (34), and (35) in to Eq. (B2) we rewrite the latter in a form similar to Eq. (B4)

$$\left(\frac{K_{-1}}{\omega} + K_0 + K_1\omega + K_2\omega^2\right) M_2^{\rm BDH}(\omega,Q^2) = \left(\frac{K_{-1}}{\omega} + K_0 + K_1\omega + K_2\omega^2\right) \times D\left[A_0\frac{1}{\omega} + A_1\left(\frac{1}{\omega^2} + \frac{L_1}{\omega}\right) + A_2\left(\frac{2}{\omega^3} + \frac{2L_1}{\omega^2} + \frac{L_1^2}{\omega}\right)\right]. \qquad \text{(B5)}$$

Now, equating in Eqs. (B4) and (B5) the corresponding coefficients in front of ω^{-k} we obtain

$$K_{-1} = 3, \qquad K_0 = -L_1 - \frac{A_1}{2A_2}, \qquad K_1 = -\frac{A_0}{A_2} + \frac{A_1^2}{4A_2^2},$$
$$K_2 = \frac{1}{2}L_1^3 + \frac{3A_1}{4A_2}L_1^2 + \frac{3A_0}{2A_2}L_1 + \frac{3A_0A_1}{4A_2^2} - \frac{A_1^3}{8A_2^3}. \qquad \text{(B6)}$$

[1] A. M. Cooper-Sarkar, R. C. E. Devenish, and A. De Roeck, Int. J. Mod. Phys. A **13**, 3385 (1998); A. V. Kotikov, Phys. Part. Nucl. **38**, 1 (2007); **38**, 828 (2007).
[2] M. Gluck, E. Reya, and A. Vogt, Z. Phys. C **67**, 433 (1995).
[3] M. Gluck, E. Reya, and A. Vogt, Eur. Phys. J. C **5**, 461 (1998); M. Gluck, P. Jimenez-Delgado, and E. Reya, Eur. Phys. J. C **53**, 355 (2008); P. Jimenez-Delgado and E. Reya, Phys. Rev. D **79**, 074023 (2009); M. Gluck, C. Pisano, and

E. Reya, Phys. Rev. D **77**, 074002 (2008); Eur. Phys. J. C **50**, 29 (2007).

[4] P. Jimenez-Delgado and E. Reya, Phys. Rev. D **89**, 074049 (2014).

[5] C. Pisano, Nucl. Phys. B, Proc. Suppl. **191**, 35 (2009); **186**, 47 (2009).

[6] S. Dulat, T.-J. Hou, J. Gao, M. Guzzi, J. Huston, P. Nadolsky, J. Pumplin, C. Schmidt, D. Stump, and C.-P. Yuan, Phys. Rev. D **93**, 033006 (2016); L. A. Harland-Lang, A. D. Martin, P. Motylinski, and R. S. Thorne, Eur. Phys. J. C **75**, 204 (2015); A. Accardi, L. T. Brady, W. Melnitchouk, J. F. Owens, and N. Sato, Phys. Rev. D **93**, 114017 (2016); S. Alekhin, J. Blmlein, S. Moch, and R. Placakyte, Phys. Rev. D **96**, 014011 (2017).

[7] R. D. Ball, V. Bertone, M. Bonvini, S. Marzani, J. Rojo, and L. Rottoli, Eur. Phys. J. C **78**, 321 (2018).

[8] H. Abdolmaleki *et al.* (xFitter Developers' Team), Eur. Phys. J. C **78**, 621 (2018).

[9] E. G. De Oliveira, A. D. Martin, and M. G. Ryskin, Phys. Rev. D **97**, 074021 (2018).

[10] V. S. Fadin, E. A. Kuraev, and L. N. Lipatov, Phys. Lett. **60B**, 50 (1975); E. A. Kuraev, L. N. Lipatov, and V. S. Fadin, Sov. Phys. JETP **44**, 443 (1976); **45**, 199 (1977); I. I. Balitsky and L. N. Lipatov, Sov. J. Nucl. Phys. **28**, 822 (1978).

[11] A. V. Kotikov and G. Parente, Nucl. Phys. **B549**, 242 (1999); G. Cvetic, A. Yu. Illarionov, B. A. Kniehl, and A. V. Kotikov, Phys. Lett. B **679**, 350 (2009).

[12] M. Froissart, Phys. Rev. **123**, 1053 (1961).

[13] E. L. Berger, M. M. Block, and C. I. Tan, Phys. Rev. Lett. **98**, 242001 (2007); M. M. Block, E. L. Berger, and C. I. Tan, Phys. Rev. Lett. **97**, 252003 (2006).

[14] M. M. Block, L. Durand, P. Ha, and D. W. McKay, Phys. Rev. D **84**, 094010 (2011); **88**, 014006 (2013).

[15] M. M. Block, L. Durand, and P. Ha, Phys. Rev. D **89**, 094027 (2014).

[16] A. Y. Illarionov, B. A. Kniehl, and A. V. Kotikov, Phys. Rev. Lett. **106**, 231802 (2011); M. M. Block, L. Durand, P. Ha, and D. W. McKay, Phys. Rev. D **88**, 013003 (2013).

[17] C. A. Argelles, F. Halzen, L. Wille, M. Kroll, and M. H. Reno, Phys. Rev. D **92**, 074040 (2015).

[18] A. Bhattacharya, R. Enberg, Y. S. Jeong, C. S. Kim, M. H. Reno, I. Sarcevic, and A. Stasto, J. High Energy Phys. 11 (2016) 167.Y. S. Jeong, M. V. Luu, M. H. Reno, and I. Sarcevic, Phys. Rev. D **96**, 043003 (2017).

[19] R. Gandhi, C. Quigg, M. H. Reno, and I. Sarcevic, Astropart. Phys. **5**, 81 (1996); Phys. Rev. D **58**, 093009 (1998); L. A. Anchordoqui, A. M. Cooper-Sarkar, D. Hooper, and S. Sarkar, Phys. Rev. D **74**, 043008 (2006).

[20] L. A. Anchordoqui, C. Garca Canal, and J. F. Soriano, arXiv:1902.10134.

[21] V. N. Gribov and L. N. Lipatov, Sov. J. Nucl. Phys. **15**, 438 (1972); L. N. Lipatov, Sov. J. Nucl. Phys. **20**, 94 (1975); G. Altarelli and G. Parisi, Nucl. Phys. **B126**, 298 (1977); Y. L. Dokshitzer, Sov. Phys. JETP **46**, 641 (1977).

[22] A. V. Kotikov, JETP Lett. **59**, 667 (1994); A. V. Kotikov and G. Parente, Phys. Lett. B **379**, 195 (1996).

[23] A. V. Kotikov, J. Exp. Theor. Phys. **80**, 979 (1995); A. V. Kotikov and G. Parente, Mod. Phys. Lett. A **12**, 963 (1997); J. Exp. Theor. Phys. **85**, 17 (1997).

[24] G. Altarelli and G. Martinelli, Phys. Lett. **76B**, 89 (1978).

[25] A. V. Kotikov, Phys. Rev. D **49**, 5746 (1994); Phys. Atom. Nucl. **57**, 133 (1994).

[26] L. P. Kaptari, A. V. Kotikov, N. Y. Chernikova, and P. Zhang, arXiv:1812.00361.

[27] F. D. Aaron *et al.* (H1 and ZEUS Collaborations), J. High Energy Phys. 01 (2010) 109.

[28] G. R. Boroun, Phys. Rev. C **97**, 015206 (2018).

[29] A. Cooper-Sarkar and S. Sarkar, J. High Energy Phys. 01 (2008) 075; A. Cooper-Sarkar, P. Mertsch, and S. Sarkar, J. High Energy Phys. 08 (2011) 042; A. Connolly, R. S. Thorne, and D. Waters, Phys. Rev. D **83**, 113009 (2011); M. Benzke, M. V. Garzelli, B. Kniehl, G. Kramer, S. Moch, and G. Sigl, J. High Energy Phys. 12 (2017) 021.

[30] V. Bertone, R. Gauld, and J. Rojo, J. High Energy Phys. 01 (2019) 217.

[31] M. G. Aartsen *et al.* (IceCube Collaboration), Nature (London) **551**, 596 (2017).

[32] M. Bustamante and A. Connolly, Phys. Rev. Lett. **122**, 041101 (2019).

[33] M. G. Aartsen *et al.* (IceCube Collaboration), arXiv:1412.5106.

[34] L. V. Gribov, E. M. Levin, and M. G. Ryskin, Phys. Rep. **100**, 1 (1983); A. H. Mueller and J. w. Qiu, Nucl. Phys. **B268**, 427 (1986); A. H. Mueller, Nucl. Phys. **B335**, 115 (1990).

[35] W. Zhu, Nucl. Phys. **B551**, 245 (1999); W. Zhu and J. h. Ruan, Nucl. Phys. **B559**, 378 (1999); W. Zhu, J. h. Ruan, J. f. Yang, and Z. q. Shen, Phys. Rev. D **68**, 094015 (2003).

[36] R. Fiore, L. L. Jenkovszky, A. V. Kotikov, F. Paccanoni, A. Papa, and E. Predazzi, Phys. Rev. D **71**, 033002 (2005); **68**, 093010 (2003); **73**, 053012 (2006).

[37] N. Y. Chernikova and A. V. Kotikov, JETP Lett. **105**, 223 (2017); A. V. Kotikov, Phys. At. Nucl. **80**, 572 (2017).

[38] E. G. Floratos, C. Kounnas, and R. Lacaze, Nucl. Phys. **192**, 417 (1981).

[39] D. I. Kazakov and A. V. Kotikov, Nucl. Phys. **B307**, 721 (1988); **B345**, 299 (1990); D. I. Kazakov, A. V. Kotikov, G. Parente, O. A. Sampayo, and J. Sánchez Guillén, Phys. Rev. Lett. **65**, 1535 (1990); **65**, 2921 (1990).

[40] D. I. Kazakov and A. V. Kotikov, Phys. Lett. B **291**, 171 (1992).

[41] E. B. Zijlstra and W. L. van Neerven, Nucl. Phys. **B383**, 525 (1992); Phys. Lett. B **272**, 127 (1991); **273**, 476 (1991).

[42] A. V. Kotikov and V. N. Velizhanin, arXiv:hep-ph/0501274.

[43] V. A. Matveev, R. M. Muradian, and A. N. Tavkhelidze, Lett. Nuovo Cimento **7**, 719 (1973); S. J. Brodsky and G. R. Farrar, Phys. Rev. Lett. **31**, 1153 (1973); S. J. Brodsky, J. Ellis, E. Gardi, M. Karliner, and M. A. Samuel, Phys. Rev. D **56**, 6980 (1997).

[44] K. G. Chetyrkin, B. A. Kniehl, and M. Steinhauser, Phys. Rev. Lett. **79**, 2184 (1997); Nucl. Phys. **B510**, 61 (1998).

[45] S. Chekanov *et al.* (ZEUS Collaboration), Eur. Phys. J. C **21**, 443 (2001).

[46] A. Y. Illarionov, A. V. Kotikov, and G. Parente Bermudez, Phys. Part. Nucl. **39**, 307 (2008).

[47] V. Andreev *et al.* (H1 Collaboration), Eur. Phys. J. C **74**, 2814 (2014).

[48] A. V. Kotikov, A. V. Lipatov, and N. P. Zotov, J. Exp. Theor. Phys. **101**, 811 (2005).

[49] S. Catani, M. Ciafaloni, and F. Hautmann, Phys. Lett. B **242**, 97 (1990); Nucl. Phys. **B366**, 135 (1991); J. C. Collins and R. K. Ellis, Nucl. Phys. **B360**, 3 (1991); E. M. Levin, M. G. Ryskin, Y. M. Shabelski, and A. G. Shuvaev, Sov. J. Nucl. Phys. **53**, 657 (1991).

[50] B. Andersson *et al.* (Small × Collaboration), Eur. Phys. J. C **25**, 77 (2002).

[51] R. D. Ball *et al.* (NNPDF Collaboration), Eur. Phys. J. C **77**, 663 (2017).

[52] S. Alekhin *et al.*, Eur. Phys. J. C **75**, 304 (2015); F. D. Aaron *et al.* (H1 Collaboration), Eur. Phys. J. C **64**, 561 (2009).

[53] H. Abramowicz *et al.* (H1 and ZEUS Collaborations), Eur. Phys. J. C **75**, 580 (2015).

[54] M. Bonvini, S. Marzani, and T. Peraro, Eur. Phys. J. C **76**, 597 (2016); M. Bonvini, S. Marzani, and C. Muselli, J. High Energy Phys. 12 (2017) 117.

[55] F. Caola, S. Forte, and J. Rojo, Phys. Lett. B **686**, 127 (2010); Nucl. Phys. **A854**, 32 (2011).

[56] M. Bonvini and F. Giuli, arXiv:1902.11125.

[57] A. V. Kotikov, A. V. Lipatov, and N. P. Zotov, Eur. Phys. J. C **27**, 219 (2003).

[58] I. Abt, A. M. Cooper-Sarkar, B. Foster, V. Myronenko, K. Wichmann, and M. Wing, Phys. Rev. D **94**, 034032 (2016).

[59] R. Gauld and J. Rojo, Phys. Rev. Lett. **118**, 072001 (2017).

[60] A. V. Kotikov, Phys. Lett. B **338**, 349 (1994); JETP Lett. **59**, 1 (1995).

[61] A. V. Kotikov and B. G. Shaikhatdenov, Phys. Part. Nucl. **44**, 543 (2013); AIP Conf. Proc. **1606**, 159 (2014); Phys. At. Nucl. **78**, 525 (2015); Phys. Part. Nucl. **48**, 829 (2017).

[62] S. J. Brodsky, V. S. Fadin, V. T. Kim, L. N. Lipatov, and G. B. Pivovarov, JETP Lett. **70**, 155 (1999); **76**, 249 (2002).

[63] A. Y. Illarionov, B. A. Kniehl, and A. V. Kotikov, Phys. Lett. B **663**, 66 (2008); A. Y. Illarionov and A. V. Kotikov, Phys. At. Nucl. **75**, 1234 (2012).

[64] H. Abramowicz *et al.* (H1 and ZEUS Collaborations), Eur. Phys. J. C **78**, 473 (2018).

[65] A. V. Kotikov, A. V. Lipatov, G. Parente, and N. P. Zotov, Eur. Phys. J. C **26**, 51 (2002).

[66] M. H. Reno, J. F. Krizmanic, and T. M. Venters, arXiv:1902.11287; D. A. Fagundes, R. R. Francisco, and E. G. de Oliveira, arXiv:1903.05607.

[67] L. A. Anchordoqui, arXiv:1807.09645; D. d'Enterria, arXiv:1902.09505.

[68] A. Accardi *et al.*, Eur. Phys. J. A **52**, 268 (2016).

[69] J. Fleischer, A. V. Kotikov, and O. L. Veretin, Nucl. Phys. **B547**, 343 (1999).

[70] G. Cvetic and A. V. Kotikov, J. Phys. G **39**, 065005 (2012).